ELSEVIER

Biophysical Chemistry 95 (2002) 79–90

Biophysical Chemistry

www.elsevier.com/locate/bpc

Modulation of cyclin-dependent kinase 4 by binding of magnesium (II) and manganese (II)

Gaochao Tian[a,1,*], Laurie S. Kane[a], William D. Holmes[b], Stephen T. Davis[c]

[a]*Department of Molecular Biochemistry, GlaxoSmithKline Research and Development, Research Triangle Park, NC 27709, USA*
[b]*Department of Molecular Sciences, GlaxoSmithKline Research and Development, Research Triangle Park, NC 27709, USA*
[c]*Department of Cancer Biology, GlaxoSmithKline Research and Development, Research Triangle Park, NC 27709, USA*

Received 18 May 2001; received in revised form 29 November 2001; accepted 4 December 2001

Abstract

All kinases require an essential divalent metal for their activity. In this study, we investigated the metal dependence of cyclin-dependent kinase 4 (CDK4). With Mg^{2+} as the essential metal and MgATP being the variable substrate, the maximum velocity, V, was not affected by changes in metal concentration, whereas V/K was perturbed, indicating that the metal effects were mainly derived from a change in the K_m for MgATP. Analysis of the metal dependence of initial rates according to a simple metal binding model indicated the presence on enzyme of one activating metal-binding site with a dissociation constant, $K_{d(a)}$, of 5 ± 1 mM, and three inhibitory metal-binding sites with an averaged dissociation constant, $K_{d(i)}$, of 12 ± 1 mM and that the binding of metal to the activating and inhibitory sites appeared to be ordered with binding of metal to the activating site first. Substitution of Mn^{2+} for Mg^{2+} yielded similar metal dependence kinetics with a value of 1.0 ± 0.1 and 4.7 ± 0.1 for $K_{d(a)}$ and $K_{d(i)}$, respectively. The inhibition constants for the inhibition of CDK4 by MgADP and a small molecule inhibitor were also perturbed by Mg^{2+}. $K_{d(a)}$ values estimated from the metal variation of the inhibition of CDK4 by MgADP (6 ± 3 mM) and a small molecule inhibitor (3 ± 1 mM), were in good agreement with the $K_{d(a)}$ value (5 ± 1 mM) obtained from the metal variation of the initial rate of CDK4. By using the van't Hoff plot, the temperature dependence of $K_{d(a)}$ and $K_{d(i)}$ yielded an enthalpy of -6.0 ± 1.1 kcal/mol for binding of Mg^{2+} to the activating site and -3.2 ± 0.6 kcal/mol for Mg^{2+} binding to the inhibitory sites. The values of associated entropy were also negative, indicating that these metal binding reactions were entirely enthalpy-driven. These data were consistent with metal binding to multiple sites on CDK4 that perturbs the enzyme structure, modulates the enzyme activity, and alters the affinities of inhibitor for the metal-bound enzyme species. However, the affinities of small molecule inhibitors for CDK4 were not affected by the change of metal from Mg^{2+} to Mn^{2+}, suggesting that the structures of enzyme–Mg^{2+} and enzyme–Mn^{2+} were similar.

Keywords: CDK4; Protein kinase; Metal-dependent kinetics

Abbreviations: ATP, adenosine 5′-triphosphate; BSA, bovine serum albumin; CDK4, cyclin-dependent kinase 4; DMSO, dimethyl sulfoxide; EGFR, epidermal growth factor receptor; FGFR, fibroblast growth factor receptor; GST, glutathione *S*-transferase; HEPES, *N*-(2-hydroxyehtyl)piperazine-*N*′-(2-ehtanesulfonic acid); IR, insulin receptor; PKA, protein kinase A; RCM-L, carcoxyymethylated-maleylated, reduce lysozyme; SDS, sodium dodecyl sulfate; TK, tyrosine kinase; **1**, 8-[(1*H*-indazol-5-ylamino)methylene]-6,8-dihydro-7*H*-[1,3]thiazolo[5,4-*e*]indol-7-one

* Corresponding author. Tel.: +1-302-886-3178; fax: +1-302-886-4983.
E-mail address: gaochao.tian@astrazeneca.com (G. Tian).
[1] Current address: Department of Lead Discovery, AstraZeneca Research and Development, 1800 Concord Pike, Wilmington, DE 19850, USA.

0301-4622/02/$ - see front matter
PII: S0301-4622(01)00251-4

1. Introduction

Protein kinases are crucial components of the signal transduction pathways that are central to cellular and biological functions [1,2]. Consequently, genetic or somatic changes that activate protein kinases are frequently responsible for the development of such detrimental diseases as diabetes, rheumatoid arthritis, and cancer [3–6] and targeting protein kinases is currently a popular approach taken by pharmaceutical industry for developing effective treatments of these diseases. Currently, approximately 500 protein kinases have been discovered and as many as 2500 protein kinases have been estimated to exist [7–9]. Over the past decade, tremendous progress has been made toward understanding of the kinetics, structures, and mechanisms of protein kinases, and in developing potent and selective protein kinase inhibitors as potential therapeutics.

All kinases require an essential divalent metal cation for their activity. An accepted role of the divalent metal is that it complexes nucleotide, such as ATP, in order to form the active, metal–nucleotide substrate [10–13]. This metal–nucleotide interaction is mainly bidendate where the metal coordinates with the β, γ and probably to a lesser degree, α-phosphoryl groups of the nucleotide [14,15]. The metal–nucleotide interaction neutralizes charge, orients and polarizes the γ-phosphoryl group and thereby, facilitates a facile phosphoryl transfer during the enzyme-catalyzed phosphotransfer reactions [13,16]. In the case of PKA, Mg^{2+} can contribute as much as a factor of 300 to catalysis [16], demonstrating the importance of the metal–nucleotide interaction. Without being associated with a divalent metal, the free nucleotide is not a substrate and can function as a competitive inhibitor [17,18].

A less understood role of the divalent metal is its modulation of enzyme activity through binding to enzyme allosteric sites [10]. This mode of enzyme regulation has been proposed for kinases catalyzing phosphoryl transfer reactions with small biochemical substrates, such as choline kinase [19] and pyruvate kinase [20], as well as for protein tyrosine kinases, such as IR TK [21,22], EGFR TK [23], FGFR TK [24], Csk [24], and Src [24]. Binding metal to enzyme allosteric sites has also been observed for PKA [25–27], a serine/threonine protein kinase, and this binding is inhibitory [26,27].

In the current study, kinetic and thermodynamic analyses of the metal requirement of cyclin-dependent kinase 4 (CDK4), a serine/threonine protein kinase, were performed. The data presented here are consistent with metal binding to multiple sites on enzyme that likely perturbs the enzyme structure, activates as well as inhibits the enzyme activity dependent upon the allosteric sites the metals bind, and alters the affinity of inhibitors for the metal-bound enzyme species.

2. Methods and experimental procedures

2.1. Materials

ATP, $MgCl_2$, $MnCl_2$, DTT, BSA, HEPES and *p*-aminobenzamidine were of reagent grade from Sigma. [γ-^{33}P]ATP (10 mCi/ml) was from Amersham. Stock solutions of GST-Rb and ATP were prepared in 100 mM HEPES, pH 7.5. 1 M $MgCl_2$ and $MnCl_2$ stock solutions were prepared in H_2O and the actual concentrations were determined by atomic absorption spectroscopy. Ni-chelating Sepharose FF resins were from Pharmacia.

2.2. Expression and purification of D1-CDK4 fusion protein

The enzyme used in this study was a cyclin D1 and CDK4 fusion protein constructed by fusing cyclin D1 to the N-terminus of CDK4 with a 16 residue linker (GGGGGSGGGGSGGGGS). This fusion protein was expressed from baculovirus and purified using a Ni-chelating Sepharose FF column and an anion exchange column (Q-Sepharose HP). The purity (>95%) was assessed by using SDS-PAGE. The purified protein was aliquoted and frozen at −80 °C before use.

2.3. Expression and purification of GST-Rb

GST-Rb used in this study was constructed by fusing GST to the N-terminus of a truncated Rb

protein that contained amino acid residues of Rb from 773 to the end. This protein was expressed in *E. coli* and purified by using a glutathione Sepharose 4B column and a Poros HS column. The purity (>95%) of the protein was estimated by using SDS-PAGE. The purified protein was aliquoted and frozen at −80 °C before use.

2.4. Radioactive glutathione plate-binding assay of CDK4

Fifty microliter reaction mixtures containing 100 mM HEPES, pH 7.5, 1 μCi/ml [γ-^{33}P]ATP, 0.5 μM GST-RB protein, 10 mM $MgCl_2$, 2.5 mM EDTA, 0.2 mg/ml BSA, 1 mM DTT and 7.5 nM CDK4/cyclinD1 enzyme, were prepared in a 96-well polystyrene plate. The reactions were started by addition of enzyme and quenched after 30 min of incubation by addition of 50 μl 100 mM EDTA, pH 8.0, and 2 μM ATP. One hundred microliters of a quenched reaction mixture was transferred to a glutathione-coated 96-well plate, and incubated at room temperature (22 °C) overnight to allow complete binding of the GST-RB protein to glutathione. The glutathione-coated plate was then washed in a 96-well plate washer with 4×150 μl /well de-ionized H_2O. Following washing 150 μl /well Ultina-Flo M scintillant was added and the plate was sealed with a plastic plate sealer. The radioactivity of each well of the plate was then determined in a micro-β plate counter (Wallac).

2.5. K_m (ATP) determination of CDK4

Fifty microliter reaction mixtures containing 100 mM HEPES, pH 7.5, 20 μCi/ml [γ-^{33}P]ATP, 0.5 μM GST-RB protein, 10 mM $MgCl_2$, 2.5 mM EDTA, 0.2 mg/ml BSA, 1 mM DTT and 15 nM D1-CDK4, were prepared in a 96-well polystyrene plate. ATP concentration was varied from 500 μM final reaction concentration to 0.5 μM final reaction concentration by two-fold serial dilution. The reactions were quenched with 50 μl 2.5% TCA after being incubated for 30 min at room temperature (22 °C). The reactions were transferred to a filter binding plate (Millipore) and washed three times with 1% H_3PO_4. Ten microliters of Scintiverse BD was then added to each well and the radioactivity of each well of the plate was determined in a micro-β plate counter. The cpms as a function of [ATP] were fit to Eq. (1) using non-linear squares analysis to estimate $K_{m(ATP)}$, the K_m-value for ATP.

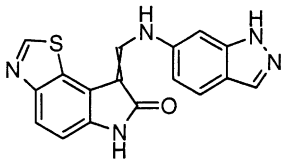

1

Scheme 1.

2.6. Inhibition of CDK4

The reactions were carried out and processed as described above. Structure **1** (Scheme 1) was prepared at a 2-μM final reaction concentration and two-fold serial-diluted in pure DMSO and then transferred to assay plates. The transferred volume was such that the final DMSO in each reaction was 2%. ADP was prepared in 100 mM HEPES, pH 7.5 and two-fold serial-diluted before being transferred to an assay plate. The activities of D1-CDK4 in the presence of inhibitor were determined in the same way as described above. The IC_{50} values were obtained by fitting data to Eq. (2) using non-linear squares analysis as described in Section 2.9 below.

2.7. Metal dependence of CDK4

The reactions were run using the procedures as described above in Section 2.4 with the metal concentration varied between 0 and 50 mM, with [ATP] = 2 μM and [GST-RB] = 0.5 μM. To determine the metal effect on V and V/K, the reactions were run at a specified metal concentration and different ATP concentrations with GST-Rb fixed at 0.5 μM. Kinetic properties of V and V/K were obtained by fitting data to Eq. (1) as described in Section 2.9 below.

2.8. Temperature-dependence of metal effect on CDK4

The assays were run according to the procedures as described above at various temperatures. The data were fitted to Eq. (13) with $n=3$ (see below in Section 2.9) by non-least squares analysis to estimate dissociation constants of metal binding. Enthalpy and entropy of metal binding were obtained by fitting the temperature-dependent dissociation constant data to Eq. (25) as described in Section 2.9 below.

2.9. Data analysis

Initial rates (υ) were analyzed by using the Michaelis–Menten equation:

$$\upsilon = \frac{V_m[S]}{K_m + [S]} \tag{1}$$

where V_m is the maximum velocity and K_m the Michaelis–Menten constant for substrate S.

The apparent inhibition constant, IC_{50}, where the enzyme activity is inhibited by inhibitor, I, by 50% was obtained by non-linear least squares analysis of data using [28]:

$$R \equiv 1 - \frac{\upsilon_i}{\upsilon} = \frac{[I]}{IC_{50} + [I]} \tag{2}$$

where υ_i is the initial rate in the presence of inhibitor. The value of IC_{50} is reduced to K_i where the substrate concentration is much less than the K_m.

To quantitate metal effects on enzyme activity, a general kinetic mechanism is illustrated as below:

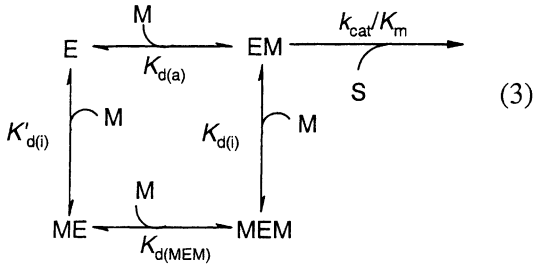

(3)

where E is enzyme, M is metal, S is substrate, EM is the enzyme–metal complex with metal bound at the activating site, and ME and MEM are enzyme complexes with a metal bound at the inhibitory site; k_{cat} is the turnover number; the equilibria are characterized by the following dissociation constants:

$$K_{d(a)} = \frac{[M][E]}{[EM]} \tag{4}$$

$$K_{d(i)} = \frac{[M][EM]}{[MEM]} \tag{5}$$

$$K'_{d(i)} = \frac{[M][E]}{[ME]} \tag{6}$$

and

$$K_{d(MEM)} = \frac{[M][ME]}{[MEM]}. \tag{7}$$

The mass balance is given by

$$E_t = [E] + [EM] + [ME] + [MEM] \tag{8}$$

where E_t represents the total concentration of enzyme. The initial velocity for this system, υ, under the V/K condition is given by

$$\upsilon = \frac{k_{cat}}{K_m}[EM][S]. \tag{9}$$

Assuming that $[M]$ is constant during the enzymatic reaction, the equilibrium system can be solved for $[EM]$ as

$$[EM] = \frac{E_t}{1 + K_{d(a)}\left(\frac{1}{K'_{d(i)}} + \frac{1}{[M]}\right) + \frac{[M]}{K_{d(i)}}} \tag{10}$$

Bringing Eq. (10) into Eq. (9), we have

$$\upsilon = \frac{\upsilon_o}{1 + K_{d(a)}\left(\frac{1}{K'_{d(i)}} + \frac{1}{[M]}\right) + \left(\frac{[M]}{K_{d(i)}}\right)} \tag{11}$$

where υ_0, the maximum initial rate, is given by

$$\upsilon_0 = \frac{k_{cat}}{K_m}E_t[S]. \tag{12}$$

Generally, if there are multiple inhibitory binding sites, Eq. (11) may be expressed as

$$\upsilon = \frac{\upsilon_0}{1 + K_{d(a)}\left(\frac{1}{K'_{d(i)}} + \frac{1}{[M]}\right) + \left(\frac{[M]}{K_{d(i)}}\right)^n} \quad (13)$$

where n is the number of the inhibitory sites. For an ordered binding of metal to the activating site and followed by binding of metal to the inhibitory site, namely, $K'_{d(i)} \gg K_{d(a)}$, Eq. (13) is reduced to:

$$\upsilon = \frac{\upsilon_o}{1 + \frac{K_{d(a)}}{[M]} + \left(\frac{[M]}{K_{d(i)}}\right)^n}. \quad (14)$$

The effects of metal binding to the activating site on the binding of inhibitor to enzyme is given by

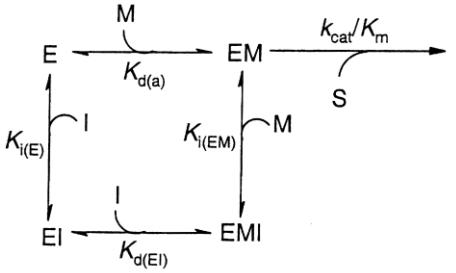

(15)

where I is inhibitor; the dissociation constants for the equilibria are given by

$$K_{i(E)} = \frac{[I][E]}{[EI]} \quad (16)$$

$$K_{i(EM)} = \frac{[I][EM]}{[EMI]} \quad (17)$$

$$K_{d(a)} = \frac{[M][E]}{[EM]} \quad (18)$$

and

$$K_{d(EM)} = \frac{[M][EI]}{[EMI]}. \quad (19)$$

The mass balance is given by

$$E_t = [E] + [EI] + [EM] + [EMI]. \quad (20)$$

Assuming $[I]$ and $[M]$ are constant during the enzymatic reaction, the equilibrium system can be solved for $[EM]$ as

$$[EM] = \frac{E_t}{\frac{K_{d(a)}}{[M]}\left(1 + \frac{[I]}{K_{i(E)}}\right) + \left(1 + \frac{[I]}{K_{i(EM)}}\right)}. \quad (21)$$

Bringing Eq. (21) into Eq. (9), we have

$$\upsilon = \frac{\upsilon_o}{\frac{K_{d(a)}}{[M]}\left(1 + \frac{[I]}{K_{i(E)}}\right) + \left(1 + \frac{[I]}{K_{i(EM)}}\right)}. \quad (22)$$

Rearranging yields:

$$\upsilon = \frac{\upsilon_o}{1 + \frac{[I]}{(K_i)_{app}}} \quad (23)$$

where the apparent inhibition constant $(K_i)_{app}$ is given by

$$(K_i)_{app} = K_{i(EM)} \frac{K_{d(a)} + [M]}{K_{d(a)} \frac{K_{i(EM)}}{K_{i(E)}} + [M]}. \quad (24)$$

Enthalpy (ΔH) and entropy (ΔS) for metal binding were obtained by a linear squares fitting of dissociation constants K_d ($K_{d(a)}$ and $K_{d(i)}$) values determined at different temperatures to the van't Hoff plot:

$$-R\ln\frac{1}{K_d} = \Delta H\frac{1}{T} - \Delta S \quad (25)$$

where R is the gas constant, and T the temperature in K.

3. Results

3.1. Effects of metal binding on the CDK4 enzymatic activity

The initial rates of CDK4 as a function of Mg^{2+} are shown in Fig. 1. The reactions were run at ATP concentrations much less than the K_m for MgATP (18 μM, data not shown) and therefore, the variation of the CDK4 activity by metal concentration indicated perturbation of the V/K. To evaluate if V was also affected, both V and V/K were determined at various $[Mg^{2+}]$ values. As

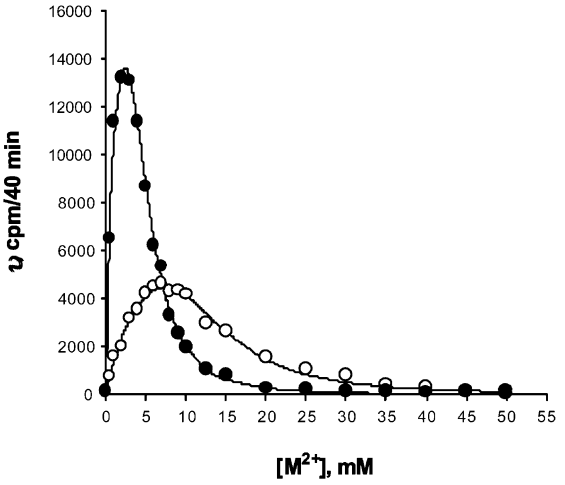

Fig. 1. Plots of the initial rate, υ, of the CDK4-catalyzed reaction as a function of the concentration of divalent metals (M^{2+}), [Mg^{2+}] (○) or [Mn^{2+}] (●) at pH 7.5, 22 °C. The solid lines are theoretical values calculated by using Eq. (13) with $n=3$ and the kinetic parameters given in Table 1.

shown in Fig. 2, [Mg^{2+}] had no effect on V (Fig. 2a) but had an effect on V/K (Fig. 2b). The metal effect on V/K (Fig. 2b) was similar to the effect on the initial rate obtained at low concentrations of ATP (Fig. 1). These data indicate that the metal effects were mainly from a change in K_m.

A simple model (Eq. (3)) assuming that the metal effects were due to direct binding of metal to enzyme was formulated (see Section 2) to provide a quantitative understanding of the metal effects. An initial analysis of data according to Eq. (13) suggested an ordered binding of metal to enzyme metal binding sites with binding of metal to an activating site first ($K_{d(i)} \gg K_{d(a)}$) (data not shown). The data were then re-analyzed using Eq. (15) by choosing only integrals for n. The best fit of data was consistent with the presence of one activating metal-binding site and three inhibitory metal-binding sites. As shown in Table 1, the dissociation constants for Mg^{2+} binding to the activating site, $K_{d(a)}=5\pm1$ mM, and the inhibitory sites, $K_{d(i)}=12\pm1$, obtained at low [ATP] agreed well with the values 6 ± 3 and 11 ± 2, respectively, obtained from metal variation of V/K. These values are much greater than the dissociation constants for MgATP (20 μM) [29] and therefore, cannot be attributed to binding of metal to ATP. The activation of enzyme observed for Mg^{2+} concentrations up to 10 mM is clearly attributable to lowing K_m upon the metal binding to the activating site. The pattern of initial rates obtained with Mn^{2+} was similar to the pattern obtained with Mg^{2+} (Fig. 1). The differences were mainly two-fold: (1) the maximum activity, υ_0, in the presence of Mn^{2+} was much greater than υ_0 in the presence of Mg^{2+}; and (2) the binding of Mn^{2+} to enzyme was tighter than the binding of Mg^{2+} (Table 1). These data are consistent with

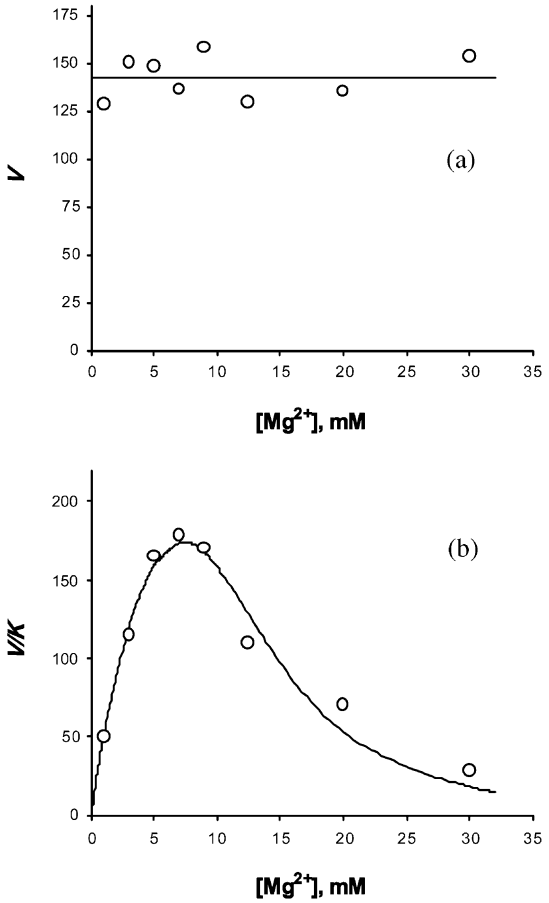

Fig. 2. Pots of the maximum velocity, V (a), and the first order rate, V/K (b) of the CDK4-catalyzed reaction as a function of [Mg^{2+}]. The solid line in panel A is the average of all the data shown in the figure. The solid line in b was calculated using Eq. (13) with $n=3$ and the kinetic parameters given in Table 1.

Table 1
Constants for divalent metal-binding to CDK4 measured at pH 7.5, 22 °C

Metal	v_0 (cpm/min)	$K_{d(a)}$ (μM)	$K_{d(i)}$ (mM)	y
Mg^{2+} [a]	5635±591	5±1	12±1	3
Mg^{2+} [b]	255±54	6±3	11±2	3
Mn^{2+} [a]	24 380±3244	1.0±0.1	4.7±0.1	3

[a] Data obtained from metal variation of the CDK4 activity at low [MgATP].

[b] Data obtained from metal variation of V/K. The low cpm value in this measurement compared to the value obtained at low [MgATP] was due to low specific radioactivity used in this experiment.

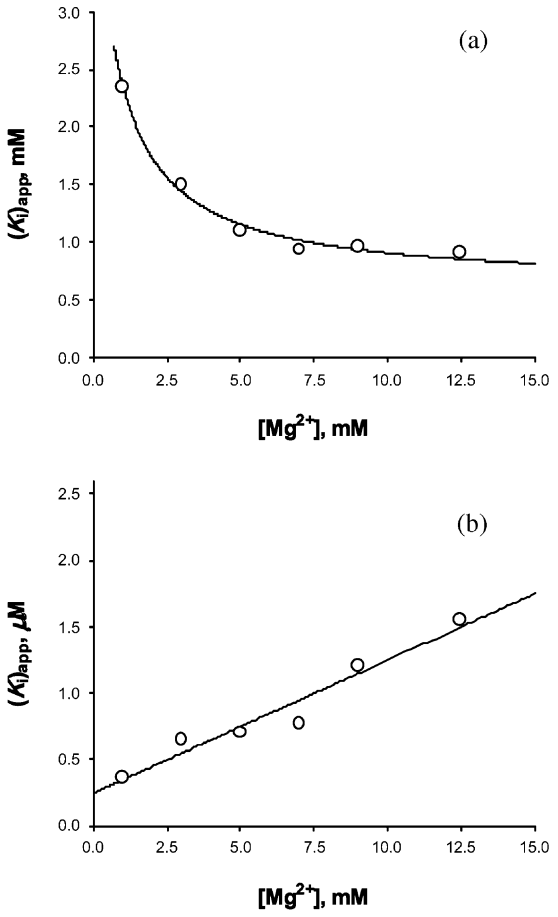

Fig. 3. Plots of the apparent inhibition constant, $(K_i)_{app}$, for ADP (a) and 1 (b) as a function of [Mg^{2+}]. The solid lines are theoretical values calculated using Eq. (24) with the parameters given in Table 2.

Table 2
Constants for inhibition of CDK4 as a function of Mg^{2+} concentration and dissociation constants for Mg^{2+}-binding to CDK4 at pH 7.5, 22 °C

Inhibitor	$K_{i(E)}$ (μM)	$K_{i(EM)}$ (μM)	$K_{d(a)}$ (mM)
ADP	$(4.6\pm1.3)\times10^{3}$	$(0.6\pm0.1)\times10^{3}$	6±3
1	$(2.5\pm1.0)\times10^{-1}$		3±1

the model [Eq. (3)] used for analyzing metal effects on the CDK4 activity that assumes metal binding to enzyme.

3.2. Effects of metal binding on the inhibition of CDK4

The above analysis assumed that the metal effects observed in Figs. 1 and 2b were due to metal binding to enzyme. If this assumption was true, one would expect similar metal effects on inhibitor binding to enzyme. Two inhibitors, ADP and 1 (Scheme 1), a small molecule inhibitor of CDK4 that is competitive vs. MgATP (data not shown), were used to evaluate this hypothesis. As shown in Fig. 3a, the apparent inhibition constant, $(K_i)_{app}$, for ADP decreased as [Mg^{2+}] increased. The effect again cannot be attributed to changes in [MgADP] for the concentrations of Mg^{2+} used in this experiment were much greater than the dissociation constant for the MgADP complex (78 μM) [29]. A model [Eq. (15)] of metal effects on inhibitor binding assuming that metal binds only to the activating site was solved. According to this model, $(K_i)_{app}$ [Eq. (23)], the apparent inhibition constant in the presence of a metal, can be expressed as a function of $K_{d(a)}$, the dissociation constant for Mg^{2+} binding to the activating site, $K_{i(EM)}$, the inhibition constant for the inhibition of the enzyme–Mg^{2+} complex (EM), and $K_{i(E)}$, the inhibition constant for the inhibition of the free enzyme (E) [Eq. (24)]. Inhibition of CDK4 by ADP was run at 1–12.5 mM Mg^{2+}, where the metal binding to the inhibitory sites was limited but sufficient for saturating the binding of metal to ADP. Analysis of the inhibition data using Eq. (23) yielded $(K_i)_{app}$ values at different Mg^{2+} concentrations (Fig. 3a). Fitting the $(K_i)_{app}$ values

according to Eq. (24) provided estimates of $K_{i(EM)}$ and $K_{i(E)}$. As shown in Table 2, this analysis indicated an eight-fold increase ($K_{i(E)}/K_{i(EM)} \cong 8$) in ADP binding to enzyme in the presence of Mg^{2+}. The presence of Mg^{2+} also affected $(K_i)_{app}$ for **1** (Fig. 3b), but metal binding increased the $(K_i)_{app}$ for **1** rather than decreasing $(K_i)_{app}$ as observed for ADP. The dissociation constant for metal binding to the activating site, $K_{d(a)}$, by this analysis [Eq. (24)] was 6 ± 3 mM from variation of $(K_i)_{app}$ for ADP (Table 2) and 3 ± 1 mM from variation of $(K_i)_{app}$ for **1** (Table 2). These values were in good agreement with the values obtained from the metal effect on the initial rates of CDK4 at low concentrations of ATP (5 ± 1 mM) (Table 1) and from the metal effect on V/K (6 ± 3 mM) (Table 1). These data suggest that the metal binding to CDK4 perturbs the enzyme structure and alters the affinities of inhibitors for the metal-bound enzyme species although other possibilities, such as metal binding at adjacent sites in or near the active site, cannot be ruled out.

3.3. Non-specific metal effects

A number of possibilities exist for non-specific metal effects. The highest divalent metal concentration used in this study was 50 mM. This translates into an ionic strength of 150 mM. To rule out the effect due to the change in ionic strength with the change in the divalent metal concentration, the activity of CDK4 at 10 mM Mg^{2+} and in the presence of 0–1 M NaCl was analyzed. This analysis indicated very little change in CDK4 activity with the concentration of NaCl (data not shown). The CDK4 used in this study was not very stable. This raised the question if the presence of a divalent metal could stabilize or destabilize the enzyme. Pre-incubation of CDK4 with 10 mM $MgCl_2$ at 4 °C for 20 min did not change the CDK4 activity, suggesting that the observed metal effects were not due to a perturbation of the enzyme stability. The fact that the $K_{d(a)}$ derived from metal effects on the inhibition of CDK4 by **1** was identical to the $K_{d(a)}$ values from metal effects on CDK4 activity (see above) also argues against non-specific effects arising from factors such as the presence of a divalent metal interacting with a contaminating CDK4 inhibitor or activator.

3.4. Temperature dependence of metal effects on the CDK4 activity

Microcalorimetry has been used extensively to study metal–protein interactions. Application of this technique to metal–CDK2 interactions revealed binding of at least two Mg^{2+} ions to this enzyme (Rocque, W., personal communication). This technique is, however, not easily amenable to studying metal binding to CDK4 because of the relatively low stability of enzyme. To gain thermodynamic insights into the metal binding to CDK4, metal effects on the CDK4 enzyme activity were examined at various temperatures (Fig. 4a). $K_{d(a)}$ and $K_{d(i)}$ (Table 3), the dissociation constants for Mg^{2+} binding to the activating and inhibitory sites, respectively, were obtained by non-linear least squares analysis of data obtained at various temperatures by using Eq. (14) with $n=3$. The $K_{d(a)}$ and $K_{d(i)}$ values as a function of temperature were then re-evaluated using the van't Hoff plot (Fig. 4b) to obtain the enthalpy (ΔH) and entropy (ΔS) of metal binding (Table 3). The negative values for both enthalpy and entropy clearly indicated that the metal binding to both the activating and inhibitory sites on CDK4 was driven by enthalpy.

3.5. Change of metal from Mg^{2+} to Mn^{2+} does not perturb inhibition of CDK4 by small molecule inhibitors

The data presented so far are consistent with metal binding of enzyme and that this binding perturbs the enzyme structure and alters the affinities of inhibitors for enzyme. We were curious to see if different metals would cause different changes in the enzyme structure and perturbs the affinities of the inhibitors. To address this question, inhibition of CDK4 by a series of small molecule inhibitors was performed in the presence of Mg^{2+} or Mn^{2+} at their optimal concentrations, and the inhibition constants obtained with Mg^{2+} were compared to those obtained in the presence of Mn^{2+}. As shown in Fig. 5, a linear correlation

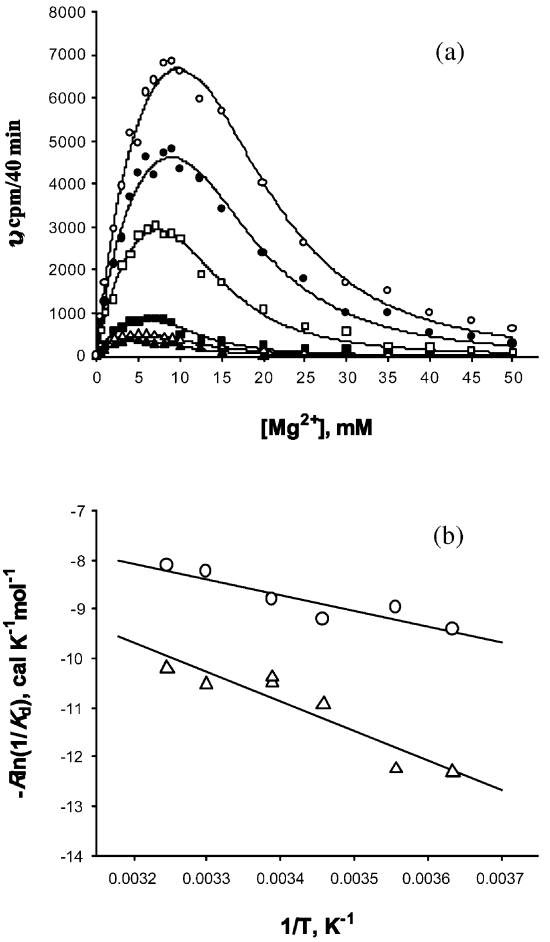

Fig. 4. (a) Plots of the initial rate, υ, of the CDK4-catalyzed reaction as a function of $[Mg^{2+}]$ at pH 7.5 and 2 (▲), 8 (△), 16 (■), 22 (□), 30 (●), and 35 (○) °C. The solid lines are theoretical values calculated using Eq. (13) and the parameters given in Table 3. (b) Plots of $-R\ln(1/K_{d(a)})$ (△) or $-R\ln(1/K_{d(i)})$ (□) as a function of $1/T$.

between the two sets of inhibition constants was evident. The fact that this linear correlation had a slope of 1.08 ± 0.03 suggests that the structures of enzyme–Mg^{2+} and enzyme–Mn^{2+} complexes accessible to the binding of inhibitors are similar.

4. Discussion

Several reports have indicated that protein tyrosine kinases can be activated by binding of a divalent metal (M^{2+}) to allosteric sites [21–24]. Data presented in the current study strongly suggest that binding of a divalent metal Mg^{2+} or Mn^{2+} to an allosteric site on CDK4, a serine/threonine kinase, also activates the enzyme. This result suggests that metal binding to enzyme allosteric sites could also be a general phenomenon for other serine/threonine protein kinases.

Quantitative analysis of the activation of CDK4 upon metal binding indicates a dissociation constant of 5 ± 1 mM for binding of Mg^{2+} to the activating site. This binding affinity appears similar to the affinity for binding of Mg^{2+} to Src and Csk as judged by comparing the curve of metal dependence of CDK4 presented here, and the curves for Src and Csk reported by Sun and Budde [24]. However, the mechanism that this activation is achieved by CDK4 appears quite different from the mechanism by Src and Csk. In the case of Csk and Src, the metal effect is on V [24], whereas in the case of CDK4 it is due to an increase in V/K. In addition, there is clearly inhibition of CDK4 at Mg^{2+} concentrations greater than 15 mM, whereas this inhibition is not observed for Src at 20 mM Mg^{2+} [24]. For Csk, the activity is not inhibited at 15 mM Mg^{2+} using poly E_4Y as the peptide substrate, and slightly inhibited using RCM–L as the peptide substrate [24]. The reason for this substrate-dependent inhibition at high metal concentrations is not clear, but may suggest metal–peptide interaction as a mechanism for the metal-mediated inhibition of Csk.

The metal dependence curve for CDK4 with Mn^{2+} is remarkably similar to the curve for Csk [24]. In both the cases, the activity increases to the maximum at approximately 2.5 mM Mn^{2+} and decreases to background at approximately 10 mM Mn^{2+}. In the case of Csk, the decrease in activity was attributed to protein precipitation visible at Mn^{2+} concentrations greater than 5 mM. In the case of CDK4, no protein precipitation was observed and no activity loss was attributable to pre-incubation of enzyme with Mn^{2+} at this 5 mM. The reason for this discrepancy is not clear.

The mechanism of activation for PKA, the only other protein serine/threonine kinase for which metal dependence has been investigated, is unique in that the metal mediated activation of enzyme is solely derived from metal binding to ATP [26,27].

All the other protein kinases investigated so far appear to require binding of an additional metal to an allosteric site in order to fully activate the enzyme [21–24] (Tian et al., this study).

The mechanism of enzyme activation by binding of divalent metals to allosteric sites is not a phenomenon restricted to protein kinases. Kinetic data suggest that this is also a general mechanism for activation of other kinases, such as choline kinase [19] and pyruvate kinase [20]. This mechanism has also been reported for ATPases such as pyruvate carboxylase [30]. In contrast to the abundant kinetic data for the presence of allosteric binding sites for divalent metal ions, there is little structural information on the nature of the metal binding sites. The only structural information regarding metal binding to allosteric sites on enzyme is from the crystal structure of PKA. A second metal is found to bridge the metal nucleotide complex with enzyme [31] and the binding of this second metal is considered inhibitory to the enzyme activity [26,27,31]. To date, no structural data exist to show metal binding at activating allosteric sites. Resolving this issue is important from the standpoint of drug discovery, since it is possible that perturbation of protein structures by metal binding to allosteric sites may alter the affinity of inhibitors for the enzyme, as it is suggested by data presented here, and therefore change the observed structure activity relationship for these inhibitors.

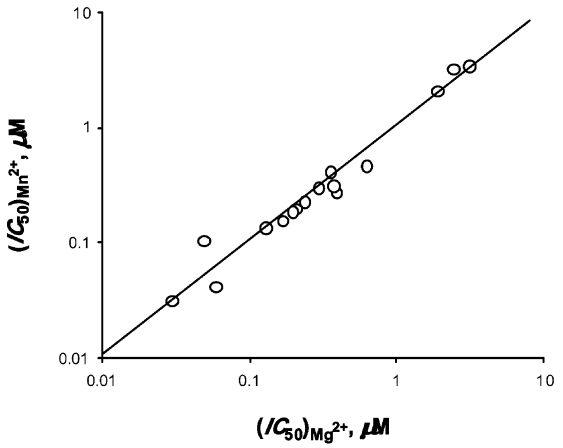

Fig. 5. Plot of IC_{50} values determined with Mn^{2+} as the activating divalent metal, $(IC_{50})_{Mn^{2+}}$, against IC_{50} values determined using Mg^{2+} as the activating metal, $(IC_{50})_{Mn^{2+}}$, for the inhibition of CDK4 by small molecule inhibitors. The linear line is from the theoretical values using a slope of 1.08 ± 0.03.

The nature of divalent metal binding to the inhibitory sites is not clear. The crystal structure of PKA with ADPPNP in the presence of Mg^{2+} indicates binding of a second metal at the ATP binding site, bridging the phosphates of ATP with enzyme [31] and this binding is inhibitory [26,27]. Since this second metal is also interacting with the phosphates of ATP, the metal ATP complex bound at the active site may be considered Mg_2ATP. It is known that Mg^{2+} can interact with ATP to form

Table 3
Effect of temperature Mg^{2+}-binding to CDK4 measured at pH 7.5

T (°C)	$1/T$ (1/°K)	v_o (cpm/min)	$K_{d(a)}$ (mM)	$K_{d(i)}$ (mM)
2	0.003634	635 ± 135	2.0 ± 0.9	8.8 ± 1.1
8	0.003556	752 ± 41	2.1 ± 0.3	11.0 ± 0.4
16	0.003458	1659 ± 340	4.1 ± 1.6	9.7 ± 1.2
22	0.003388	5635 ± 591	5.1 ± 1.0	12.0 ± 0.7
22	0.003388	5868 ± 585	5.4 ± 1.0	11.9 ± 0.7
30	0.003298	8031 ± 644	5.0 ± 0.8	15.8 ± 0.8
35	0.003245	12005 ± 791	5.9 ± 0.8	16.9 ± 0.7
Thermodynamic parameters for Mg^{2+} binding				
ΔH (kcal mol^{-1})			-6.0 ± 1.1	-3.2 ± 0.6
ΔS (cal mol^{-1} K^{-1})			-9.6 ± 3.8	-2.0 ± 2.1

Mg_2ATP in solution and such a dimetal-nucleotide species is inhibitory to kinases [18]. The current study suggests three inhibitory binding sites on CDK4 and this binding of a second metal with ATP may account for metal binding to one of the three inhibitory sites of CDK4. How the remaining two metals interact with CDK4 and inhibit the activity is totally unclear and warrants further investigations.

Divalent Mn^{2+} and Mg^{2+} are very similar in many ways [32]. They both have similar coordination numbers and angles in various coordination complexes, and function generally as a Lewis acid. However, there are subtle differences that may make these two metals behave differently. For example, Mn^{2+} has a larger radius (0.75 Å) than Mg^{2+} (0.65 Å). Generally, Mg^{2+} prefers oxygen ligands and so does Mn^{2+}, but Mn^{2+} is more acceptive of nitrogen than Mg^{2+}. These differences may account for the observed tighter binding of Mn^{2+} than Mg^{2+} in most enzymatic studies. Such differences could also result in metal binding to different allosteric sites, thereby, to perturb the enzyme structure in different ways. For drug screening against CDK4, this does not appear to be a significant concern because, as demonstrated in the current study, no differences exist in apparent inhibition constants obtained by using Mg^{2+} or Mn^{2+} in the kinase inhibition assay.

Acknowledgments

Dr Warren J. Rocque is acknowledged for sharing unpublished microcalorimetry data on metal–CDK2 binding reactions.

References

[1] T. Hunter, Protein modification: phosphorylation on tyrosine residues, Curr. Opin. Cell Biol. 1 (1989) 1168–1181.
[2] T. Hunter, Protein kinases and phosphatases: the yin and yang of protein phosphorylation and signaling, Cell 80 (1995) 225–236.
[3] P.S. Huang, D.C. Heimbrook, Oncogene products as therapeutic targets for cancer, Curr. Opin. Oncol. 9 (1997) 94–100.
[4] T. Takeuchi, T. Abe, Tyrosine phosphorylated proteins in synovial cells of rheumatoid arthritis, Int. Rev. Immunol. 17 (1998) 365–381.
[5] Y. Le Marchand-Brustel, Molecular mechanisms of insulin action in normal and insulin-resistant states, Exp. Clin. Endocrinol. Diabetes 107 (1999) 126–132.
[6] A.J. Lewis, A.M. Manning, New targets for anti-inflammatory drugs, Curr. Opin. Chem. Biol. 3 (1999) 489–494.
[7] S.T. Hanks, A.M. Quinn, T. Hunter, The protein kinase family: conserved features and deduced phylogeny of the catalytic domains, Science 241 (1988) 42–51.
[8] T. Hunter, 1001 protein kinases redux-towards 2000, Semin. Cell Biol. 5 (1994) 367–376.
[9] S.T. Hanks, T. Hunter, Protein kinases 6. The eukaryotic protein kinase superfamily: kinase (catalytic) domain structure and classification, FASEB J. 9 (1995) 576–596.
[10] B.G. Malmstrom, A. Rosenberg, Mechanism of metal ion activation of enzymes, Adv. Enzymol. Rel. Subj. Biochem. 21 (1959) 131–167.
[11] E.G. Krebs, Protein kinases, Curr. Top. Cell Regul. 5 (1972) 99–133.
[12] D.A. Walsh, E.G. Krebs, Protein kinases, Enzymes 8 (1973) 555–581.
[13] J.R. Knowles, Enzyme-catalyzed phosphoryl transfer reactions, Ann. Rev. Biochem. 49 (1980) 877–919.
[14] M. Cohn, T.R. Hughes, Nuclear magnetic resonance spectra of adenosine di- and triphosphate, J. Biol. Chem. 237 (1962) 176–181.
[15] S.L. Huang, M.-D. Tsai, Does the magnesium(II) ion interact with the alpha-phosphate of adenosine triphosphate? An investigation by oxygen-17 nuclear magnetic resonance, Biochemistry 21 (1982) 951–959.
[16] A. Mildvan, Mechanisms of signaling and related enzymes, Proteins 29 (1997) 401–416.
[17] E. James, J.F. Morrison, The reaction of nucleotide substrate analogues with denosine triphosphate-creatine phosphotransferase, J. Biol. Chem. 241 (1966) 4758–4768.
[18] J.F. Morrison, Approaches to kinetic studies on metal-activated enzymes, Methods Enzymol. 63 (1979) 257–294.
[19] J.P. Infante, J.E. Kinsella, Choline kinase kinetics studies: Dual role of Mg^{2+} in the sequential ordered mechanism at low reactant concentrations. Regulatory implications, Int. J. Biochem. 7 (1971) 483–496.
[20] A.S. Mildvan, Metals in enzyme catalysis, Enzymes 3 (1970) 445–536.
[21] M.F. White, H.U. Haring, M. Kasuga, C.R. Kahn, Kinetic properties and sites of autophosphorylation of the partially purified insulin receptor from hepatoma cells, J. Biol. Chem. 259 (1984) 255–264.
[22] P.P. Vicario, R. Saperstein, A. Bennun, Role of divalent metals in the activation and regulation of insulin receptor tyrosine kinase, BioSystems 22 (1988) 55–66.
[23] J.G. Koland, R.A. Cerione, Activation of the EGF receptor tyrosine kinase by divalent metal ions: comparison of holoreceptor and isolated kinase domain

properties, Biochim. Biophys. Acta 1052 (1990) 489–498.
[24] G. Sun, R.J.A. Budde, Csk phosphorylation and inactivation in vitro by the cAMP-dependent protein kinase, Biochemistry 36 (1997) 2139–2146.
[25] F. Huiging, J. Larner, On the mechanism of action of adenosine 3′, 5′ cyclophosphate, Proc. Natl. Acad. Sci. USA 56 (1966) 647–653.
[26] R.N. Armstrong, H. Kondo, J. Granot, E.T. Kaiser, A.S. Mildvan, Magnetic resonance and kinetic studies of the manganese(II) ion and substrate complexes of the catalytic subunit of adenosine 3′,5′-monophosphate-dependent protein kinase from bovine heart, Biochemistry 18 (1979) 1230–1238.
[27] A.S. Mildvan, P.R. Rosevear, D.C. Fry, H.N. Bramson, E.T. Kaiser, NMR studies of the mechanism of action and regulation of protein kinase, Curr. Top. Cell. Regul. 27 (1985) 133–144.
[28] G. Tian, R.A. Mook, M.L. Moss, S.V. Frye, Mechanism of time-dependent inhibition of 5α-reductases by Δ^1-4-azasteroids: toward perfection of rates of time-dependent inhibition by using ligand-binding energies, Biochemistry 34 (1995) 13453–13459.
[29] V.L. Pecoraro, J.D. Hermes, W.W. Cleland, Stability constants of Mg^{2+} and Cd^{2+} complexes of adenine nucleotides and thionucleotides and rate constants for formation and dissociation of MgATP and MgADP, Biochemistry 23 (1984) 5262–5271.
[30] W.R. McClure, H.A. Lardy, H.P. Kneifel, Rat liver pyruvate carboxylase. IV. Factors affecting the regulation in vivo, J. Biol. Chem. 246 (1971) 3569–3578.
[31] A. Madhusudan, E.A. Trafny, N.H. Xuong, , et al., cAMP-dependent protein kinase: crystallographic insights into substrate recognition and phosphotransfer, Protein Sci. 3 (1994) 176–187.
[32] C.W. Bock, A.K. Katz, G.D. Markham, J.P. Glusker, Manganese as a replacement for magnesium and zinc: functional comparison of the divalent ions, J. Am. Chem. Soc. 121 (1999) 7360–7372.